DOI: https://doi.org/10.54393/fbt.v2i01.23

FUTURISTIC BIOTECHNOLOGY

https://fbtjournal.com/index.php/fbt

Volume 2, Issue 1 (Jan-Jun 2022)

Original Article

Computational Prediction of *Cymbopogon Citratus* Compounds as Promising Inhibitors of Main Protease of SARS-CoV-2

Tuba Ahmad[1], Rashid Saif[2*], Muhammad Hassan Raza[2], Muhammad Osama Zafar[2], Saeeda Zia[3], Mehwish Shafiq[4], Laraib Ali[4] and Hooria Younas[1]

[1]Department of Biochemistry, Kinnaird College for Women, Lahore, Pakistan
[2]Decode Genomics, Punjab University Employees Housing Scheme, Lahore, Pakistan
[3]Department of Sciences and Humanities, National University of Computer and Emerging Sciences, Lahore, Pakistan
[4]Department of Biotechnology, Kinnaird College for Women, Lahore, Pakistan

ARTICLE INFO

Key Words:

SARS-CoV-2, Main Protease, COVID-19, MOE, Molecular Docking, MDS Analysis

How to Cite:

Ahmad, T., Saif, R., Hassan Raza, M., Osama Zafar, M., Zia, S., Shafiq, M., Ali, L., & Younas, H. (2022). Computational Prediction of Cymbopogon Citratus Compounds as Promising Inhibitors of Main Protease of SARS-CoV-2: Computational Prediction of Cymbopogon Citratus Compounds. Futuristic Biotechnology, 2(01). https://doi.org/10.54393/fbt.v2i01.23

***Corresponding Author:**

Rashid Saif
Decode Genomics, Punjab University Employees Housing Scheme, Lahore, Pakistan
rashid.saif37@gmail.com

Received Date: 3rd March, 2022
Acceptance Date: 6th May, 2022
Published Date: 30th June, 2022

ABSTRACT

There is a dire need to develop any antiviral therapy for the treatment of SARS-CoV-2. **Objective:** To investigate the potential therapeutic drug agents from *Cymbopogon citratus* compounds against the main-protease (M^{pro}) of SARS-CoV-2. **Methods**: Initial screening was carried out using molecular docking, dynamic simulation followed by ADMET profiling and Lipinski's physiochemical parameters for prediction of drug likeliness. MOE/PyRx was used for docking before determining the stability of the best complexes through NAMD/VMD softwares. Moreover, SwissADME and admetSAR web-based tools were used for drug likeliness of the best complexes. **Results:** Out of total 50 compounds, 11 presented the lowest binding energies which includes tannic acid, isoorientin, swertiajaponin, chlorogenic acid, cymbopogonol, warfarin, citral diethyl acetal, citral acetate, luteolin, kaempferol and cianidanol with binding energies of -8.12, -7.38, -7.33, -6.88, -6.48, -6.32, -6.31, -6.18, -6.18, -6.13 and -6.02, respectively. Current studies show isoorientin, chlorogenic acid and tannic acid as the promising drug agents using RMSD, Hbond, heatmap graphs. **Conclusion:** Further in-vivo experiments are suggested to ascertain the medicinal use of these potential inhibitors against COVID-19.

INTRODUCTION

Severe Acute Respiratory Syndrome Coronavirus 2 (SARS-CoV-2), the causative agent of COVID-19, is an enveloped positive-sense, single-stranded RNA virus that has the potential to cause infections in the respiratory, gastrointestinal, nervous, and hepatic systems in humans [1, 2]. The novel coronavirus emerged in Wuhan, China, in late 2019 during an outbreak and it belongs to the same family as Middle East Respiratory Syndrome Coronavirus (MERS) and Severe Acute Respiratory Syndrome Coronavirus (SARS-CoV) [3]. The novel coronavirus transmit human-to-human through aerosol and uses Angiotensin-converting enzyme 2 (ACE2) receptor to cause infectivity [4]. The symptoms of COVID-19 infection appear after approximately 5.2 days and include cough, fever, fatigue or myalgia, pneumonia, and dyspnea [2]. Currently, there is a lack of any antiviral therapy for the treatment of COVID-19. However, the limited measures that have been implemented include many supportive and preventive therapies to prevent organ damage and further complications [5]. The main protease, also known as

DOI: https://doi.org/10.54393/fbt.v2i01.23

3CLPro, is a key enzyme of SARS-CoV-2 that plays a major role in viral replication and transcription [6]. The Mpro processes the ORF1ab polyprotein by recognizing a specific motif sequence and producing smaller functional proteins that are essential for viral replication [7]. The M^{pro} is a potential target for designing antiviral drugs that can inhibit the enzyme's activity and prevent viral replication [8]. The $3CL^{Pro}$ is composed of anti-parallel, six-stranded β-barrels at the substrate-binding site that span through the protease-like picornavirus 3C domain II and protease-like chymotrypsin-3C domain I [9]. The dimerization process is regulated by the globular structure of five helices that are present between residues 198-303 in domain III, and this process occurs through salt bridge interactions between Arg4 and Glu290 [6, 10]. Many compounds derived from medicinal plants have been reported to have antiviral activity. One such plant is Cymbopogon citratus, commonly known as lemongrass, which belongs to the Gramineae family [11, 12]. Lemongrass possesses a range of pharmacological activities, including antimicrobial, antifungal, anti-inflammatory, antioxidant, anti-nociceptive, anti-diarrheal, and anti-obesity properties [13-15]. These properties are due to the presence of essential oils, flavonoids, phenolic compounds, and other phytochemical constituents in the herb [16, 17]. In this study, the potential inhibitors from *C. citratus* compounds were predicted against SARS-CoV-2 main-protease using molecular docking and dynamic simulation analysis. Main-protease was docked and redocked with C. citratus compounds using Molecular Docking Environment (MOE) and PyRx software to validate results. The binding energies of different compounds were calculated and potential inhibitors were scrutinized for further analysis. The stability and conformational changes of the complexes were calculated by molecular dynamic simulations using NAMD/VMD software. Additionally, the physicochemical and drug likeliness properties of the ligands was calculated using SwissADME, admetSAR and Pfizer's rule of five.

METHODS

Dataset preparation

A library of 50 compounds from *Cymbopogon citratus* was prepared having antiviral, antimicrobial, anti-fungal, anti-inflammatory, antioxidant, and anti-nociceptive properties. 3D-structures were retrieved from PubChem, DrugBank databases or by sketching on chemdraw. Prior to any analyses some preparatory changes were made in ligands structure like addition of hydrogen, assigning charges and energy minimization by universal force field (UFF) with conjugate gradient algorithm of 500 iteration. The chemical compounds of *Cymbopogon citratus* are given in Supplementary Table S1. The main protease also abbreviated as $3CL^{Pro}$, is the key enzyme in SARS-CoV-2 that has a main role in viral replication and transcription. The 3D-crystal structure of targeted protein was retrieved from Protein Data Bank (PDB ID: 6LU7). Beside the removal of repeated chains, heteroatoms, water molecules and already attached ligand, the missing hydrogen atoms were added to make correct protein conformer. Energy minimization was done with Chimera using AMBER forcefield (AMBER ff14SB). The properties of main-protease are given in Supplementary Table S2 while crystal structure is shown in Supplementary Figure S1.

Virtual library screening of Cymbopogon citratus against SARS-CoV-2 M^{pro}

Virtual screening of selected dataset was performed by MOE and PyRx to validate results. The amino acid sequence of active site of protein was either retrieved from literature or using automatic active site finder. Grid box was created with dimension of 20×20×20 Å around the active site of protein and ligand to specify docking. PyRx uses Auto-dock vina to perform docking and computing binding energy by calculating difference between the sum of energy in free state of ligand and protein and sum of energy in protein-ligand complex using AMBER3. The binding energy (ΔG) of protein-ligand interactions was calculated using following empirical equation [18].

$$\Delta G = (V^{L\text{-}L}{}_{bound} - V^{L\text{-}L}{}_{unbound}) + (V^{P\text{-}P}{}_{bound} - V^{P\text{-}P}{}_{unbound}) + (V^{P\text{-}L}{}_{bound} - V^{P\text{-}L}{}_{unbound} + \Delta S_{conf})$$

where *P* refers to the protein, *L* refers to the ligand, $V^{L\text{-}L}{}_{bound}$ energy in bounded state of ligand, $V^{L\text{-}L}{}_{unbound}$ energy in unbounded state of ligand, $V^{P\text{-}P}{}_{bound}$ energy in bounded state of protein, $V^{P\text{-}P}{}_{unbound}$ energy in unbounded state of protein, $V^{P\text{-}L}{}_{bound}$ energy in bounded state of protein and ligand, $V^{P\text{-}L}{}_{unbound}$ energy in unbounded state of protein and ligand, ΔS_{conf} denotes the loss of conformational entropy upon binding.

Calculation of properties using ADMET analysis

The pharmacokinetic and pharmacological properties of ligands which gave best binding scores were calculated to understand the pharmacokinetic role. AdmetSAR and pkCSM web-based tools were used for this purpose.

Molecular dynamic simulations of the top-scoring ligand-protein complex

The molecular dynamic (MD) simulation was performed using NAMD software to examine complex stability and flexibility by allowing to interact in virtual environment similar to human body. Ligands that gave the best docking scores against target protein and have pharmacological properties were selected for post docking analysis. The protein-ligand complex was prepared in same orientation with maximum score for simulation studies. The coordinates of best ligand having highest binding score was embedded in the protein file. The VMD software was

DOI: https://doi.org/10.54393/fbt.v2i01.23

used to build the topologies of ligand and protein to define bonds and angles, number of molecules and atom types in simulation system. The simulation inputs of ligands were built from CHARMM-GUI web server with CHARMM36 forcefield. The VMD software consists of Automatic PSF Generation which was utilized to convert the protein structure to PSF format. Afterwards, both files were merged and solvated to create a cubic box of water around the complex. Molecular dynamic simulation was run at 0.1 ns (50,000 steps). The energy minimization was done using conjugate gradient method. The periodic boundary conditions were established for energy minimized complex to run simulation. A constant temperature 310K and 1 atm pressure was established for the simulation process. After adjusting all the parameters, the MD simulation was executed using NAMD software. Afterwards, the results were analyzed by plotting histogram of RMSD, hydrogen bond and heat map.

RESULTS

Molecular docking using MOE

Molecular docking is a computational approach used to study the interactions between protein and ligands. In this study, the main protease was docked with 50 compounds of *Cymbopogon citratus* to predict the potential drug agents. The binding energies are listed in Supplementary Table S3. The negative values of binding energy define the release of energy during docking, considering the ligands having high affinity for target protein. The 2 and 3-dimensional interaction of *C. citratus* compound which gave the highest score with main protease is given in Figure 1. while rest of ligands interaction are given in Supplementary Figure S2.

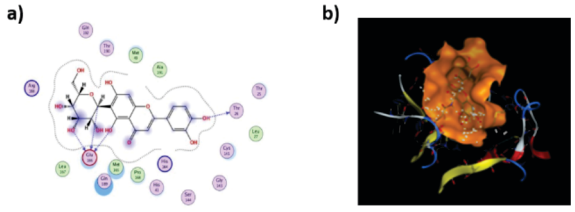

Figure 1: Two dimensional and three-dimensional interactions of Isoorientin with 6LU7

Redocking using PyRx

The three top ligands based on the lowest binding scores with M^{pro} using MOE were selected for further analysis. Before MD simulation, these ligands were first redocked with M^{pro} using PyRx to validate the results since both softwares uses different algorithms. The binding scores obtained from docking are listed in Table 1.

Compounds	Docking Scores from MOE	Docking Scores from PyRx
Tannic acid	-8.12501907	-6.6
Chlorogenic acid	-6.88325262	-6.8
Swertiajaponin	-7.33355188	-5.8
Isoorientin	-7.38438511	-6.7
Warfarin	-6.32509041	-7.5
Citral diethyl acetal	-6.30906057	-4.6
Citral acetate	-6.18121672	-5.0
Luteolin	-6.17798948	-7.1
Kaempferol	-6.13175917	-6.7
Cianidanol	-6.02349663	-6.8

Table 1: The binding energies (ΔG) of 10 compounds of C. citratus with the main protease

Drug likeliness and toxicity risk prediction

The drug likeliness attributes, pharmacokinetics and pharmacological properties of 11 compounds that gave the lowest binding scores were computed using Lipinski's rule and ADMET profiling.

Lipinski's rule of five

The Lipinski's rule physiochemical parameters were studied using the admetSAR and results are shown in Table 2. Out of 11 compounds, only tannic acid showed three violations having molecular weight, number of hydrogen bond donors, and number of hydrogen bond acceptors greater than 500Da, 5 and 10 respectively while rest of the ligands including isoorientin, swertiajaponin, chlorogenic acid and cymbopogonol showed two or less violations.

Ligand	Molecular Weight (<500Da)	logP (<5	H-Bond Donor (5)	H-Bond Acceptor (<10)	Violations
Tannic acid	636.47	-0.28	11	18	3
Isoorientin	448.38	-0.20	8	11	2
Swertiajaponin	462.40	0.10	7	11	2
Chlorogenic acid	354.31	-0.65	6	9	1
Cymbopogonol	426.72	8.02	1	1	1
Warfarin	308.33	3.61	1	4	0
Citral diethyl acetal	226.36	4.08	0	2	0
Citral acetate	210.27	2.77	0	3	0
Luteolin	286.24	2.28	4	6	0
Kaempferol	286.24	2.28	4	6	0
Cianidanol	290.27	1.55	5	6	0

Table 2: The Lipinski's physiochemical parameters of the selected compounds of C. citratus calculated by admetSAR profiling

ADMET profiling

The pharmacokinetic and pharmacological properties of 11 compounds were investigated through ADMET profiling by pkCSM as given in Table 3.

DOI: https://doi.org/10.54393/fbt.v2i01.23

Compounds	Abs.	Distribution		Metabolism							Excretion		Toxicity	
	IA (%)	VDs log (L/kg)	BBBP (Log BB)	CYP Inhibitor (Y/N)					CYP Substrate (Y/N)		Total Clearance log (ml/min/kg)	ROS (Y/N)	AMES Toxicity (Y/N)	LD50 (mol/kg)
				1A2	2C19	2C9	2D6	3A4	2D6	3A4				
Tannic acid	0.52	0.698	-3.56	N	N	N	N	N	N	N	0.417	Y	N	2.483
Isoorientin	61.76	1.603	-1.56	N	N	N	N	N	N	N	0.372	N	N	2.55
Swertiajaponin	43.48	1.204	-1.82	N	N	N	N	N	N	N	0.421	N	N	2.59
Chlorogenic acid	36.37	0.581	-1.40	N	N	N	N	N	N	N	0.307	N	N	1.973
Cymbopogonol	95.93	-0.14	0.75	N	N	N	N	N	N	Y	0.172	N	N	2.636
Warfarin	96.16	-0.266	-0.17	Y	Y	Y	N	Y	N	Y	0.719	N	N	1.773
Citral diethyl acetal	95.16	0.213	0.668	N	N	N	N	N	N	N	1.787	N	N	1.864
Citral acetate	95.24	-0.064	0.559	N	N	N	N	N	N	N	1.035	N	N	1.812
Luteolin	81.1	1.153	-0.90	Y	N	Y	N	N	N	N	0.495	N	N	2.455
Kaempferol	74.2	1.274	-0.93	Y	N	N	N	N	N	N	0.477	N	N	2.449
Cianidanol	68.82	1.027	-1.05	N	N	N	N	N	N	N	0.183	N	N	2.428

Table 3: The ADMET properties of selected compounds of C. citratus predicted by pkCSM (IA: Intestinal Absorption, VDss: Volume of Distribution in humans, BBBP: Blood-Brain Barrier Permeability, ROS: Renal Organic Cation Transporter 2 Substrate), Abs: Absorption

Furthermore, the bioavailability scores, synthetic accessibility, and other physiochemical properties of virtually screened *C. citratus* compounds were also predicted using SwissADME online tool and are listed in Table 4.

Ligand	TPSA (Å^2)	Bio-availability Score	Synthetic accessibility	Log S	Rotatable Bonds
Tannic acid	310.66	0.17	5.32	-1.624	7
Isoorientin	201.28	0.17	5.04	-2.398	3
Swertiajaponin	190.28	0.17	5.12	-2.302	4
Chlorogenic acid	164.75	0.11	4.16	-2.457	5
Cymbopogonol	20.23	0.55	5.52	-4.414	1
Warfarin	67.51	0.55	3.79	-3.953	4
Citral diethyl acetal	18.46	0.55	3.43	-3.155	8
Citral acetate	43.37	0.55	2.84	-2.918	6
Luteolin	111.13	0.55	3.02	-2.999	1
Kaempferol	111.13	0.55	3.14	-3.142	1
Cianidanol	110.38	0.55	3.50	-3.101	1

Table 4: The bioavailability scores, synthetic accessibility and physiochemical properties of virtually screened C. citratus compounds predicted by SwissADME

Molecular dynamics simulation analysis

The three compounds with highest score were selected for MD simulation due to its lowest binding energy score. The stability and flexibility of newly formed complex was examined by accessing the fluctuations in root mean square deviation (RMSD) values.

RMSD analysis

Visual Molecular Dynamics (VMD) software was used to find out the average distance between atom groups by calculating RMSD values. The RMSD graph of tannic acid in complex with 6LU7 shows quite stability from 450-850 frames with less than 0.2 Å fluctuation. The complex remained stable most of the time at 1.4 to 1.6 Å between 200-900 frames and showed comparatively greater fluctuation at the start and end of simulation while the graphs of isoorientin and chlorogenic acid complexes showed greater stability for longer intervals. The RMSD values of isoorientin complex fluctuated between 1.3Å to 1.6 Å from 25-1000 frames. An abrupt change in values can be observed in the first half between 50-500 frames, however, the second half of simulation from 500-1000 frames showed more stability with less fluctuation. The chlorogenic acid complex showed promising stability between 1.6 Å and 2 Å with less than 0.5 Å deviation from 50-1000 frames. The RMSD graphs of isoorientin, chlorogenic and tannic acids are shown in Figure 2.

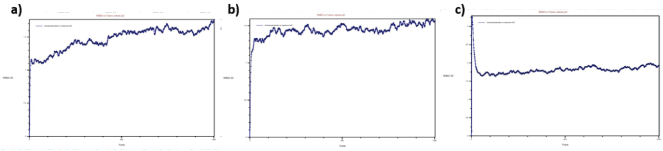

Figure 2: The RMSD graph of **a)** tannic acid **b)** isoorientin **c)** chlorogenic acid in complex with the main protease (PDB ID: 6LU7)

Analysis of hydrogen bonds

The stability of complexes was investigated by plotting histogram of hydrogen bond. The H-bond graphs of tannic acid, isoorientin and chlorogenic acid are shown in Figure 3. The formation of strong hydrogen bond reduces the gap between residues and therefore increases the stability of complex. The hydrogen bond analysis showed that tannic acid complex has total 7 hydrogen bonds, and the stability of complex is provided by the bond between ligand (donor) and Gln127 (acceptor) with 52.24% occupancy rate. Out of 7 hydrogen bonds in isoorientin complex, the bond between ligand (donor) and Glu290 (acceptor) is responsible for stability of complex which remained steady for 62.41% time of simulation process. The chlorogenic acid complex had total 10 hydrogen bonds with maximum stability due to the bond between ligand (donor) and Asp153 (acceptor with 152.94% occupancy.

DOI: https://doi.org/10.54393/fbt.v2i01.23

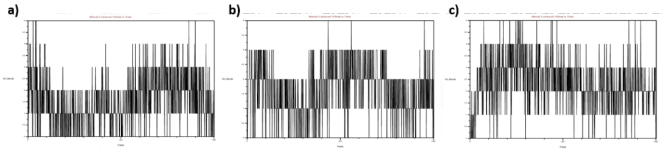

Figure 3: H-bond graph of a) tannic acid b) isoorientin c) chlorogenic acid in complex with the main protease (PDB ID: 6LU7)

Complex analysis using heat maps

The heat map plots represent the distribution of a particular property, such as the potential energy, temperature, pressure and the density of simulated system over time. The heat signatures of isoorientin and chlorogenic acid showed quite stability whereas the tannic acid depicted low stability within short intervals. The heat map graph of isoorientin, chlorogenic and tannic acids are shown in Figure 4.

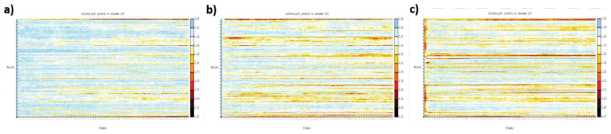

Figure 4: Heat map of **a)** tannic acid **b)** isoorientin **c)** chlorogenic acid in complex with the main protease (PDB ID: 6LU7)

DISCUSSION

The unavailability of antiviral therapy for the treatment of novel SARS-CoV-2 to date is alarming. One of the major limitations in drug discovery is due to RNA nature of its genome which mutates at a faster rate reducing the efficacy of drugs and vaccines. The present study aimed to investigate the potential therapeutic drug agents using molecular docking and dynamic simulation approaches from *Cymbopogon citratus* bioactive compounds against the main protease which is a potential drug target of SARS-CoV-2. The structures of total 50 *Cymbopogon citratus* compounds were identified and retrieved from literature and databases respectively. Their binding energies with the target protein were calculated through docking/redocking using MOE/PyRx. The stability and drug likeliness of ligands which presented lowest binding energies with viral protein was further evaluated through MDS and ADMET analysis. The *In-silico* analysis predicted isoorientin and chlorogenic acid as the potential inhibitor. Similar studies have been reported in the past in predicting the potential inhibitor of this virus. Recent study predicted the promising inhibitor against main protease from the compounds of *Olea europaea* and *Curcuma longa* [19]. Current study was limited at the computational analysis as for MDS, systems with high computation powers are required while our entire analysis was done using personal computer [20]. Analysis using system with high computation power are required to reveal the precise stability of these complexes for higher time frames.

CONCLUSIONS

In-silico drug prediction identified several potential inhibitors of SARS-CoV-2 main protease, including isoorientin, swertiajaponin, cymbopogonol, and luteolin. However, further in-vivo investigations studies are necessary to confirm the medicinal use of these potential inhibitors.

Conflicts of Interest

The authors declare no conflict of interest.

Source of Funding

The authors received no financial support for the research, authorship and/or publication of this article.

REFERENCES

[1] Pal M, Berhanu G, Desalegn C, Kandi V. Severe acute respiratory syndrome coronavirus-2 (SARS-CoV-2): an update. Cureus. 2020 Mar; 12(3): e7423. doi: 10.7759/cureus.7423.

[2] Malik YS, Sircar S, Bhat S, Sharun K, Dhama K, Dadar M, *et al*. Emerging novel coronavirus (2019-nCoV)—current scenario, evolutionary perspective based on genome analysis and recent developments. Veterinary Quarterly. 2020 Jan; 40(1): 68-76. doi: 10.1080/01652176.2020.1727993.

[3] Pachetti M, Marini B, Benedetti F, Giudici F, Mauro E, Storici P, *et al*. Emerging SARS-CoV-2 mutation hot spots include a novel RNA-dependent-RNA polymerase variant. Journal of Translational Medicine. 2020 Dec; 18: 1-9. doi: 10.1186/s12967-020-02344-6.

[4] Harrison AG, Lin T, Wang P. Mechanisms of SARS-CoV-2 transmission and pathogenesis. Trends in Immunology. 2020 Dec; 41(12): 1100-15. doi: 10.1016/j.it.2020.10.004.

[5] Peiris JS, Lai ST, Poon LL, Guan Y, Yam LY, Lim W, *et al.* Coronavirus as a possible cause of severe acute respiratory syndrome. The Lancet. 2003 Apr; 361(9366): 1319-25. doi: 10.1016/S0140-6736(03)13077-2.

[6] Chellapandi P and Saranya S. Genomics insights of SARS-CoV-2 (COVID-19) into target-based drug discovery. Medicinal Chemistry Research. 2020 Oct; 29(10): 1777-91. doi: 10.1007/s00044-020-02610-8.

[7] Jin Z, Du X, Xu Y, Deng Y, Liu M, Zhao Y, *et al.* Structure of Mpro from SARS-CoV-2 and discovery of its inhibitors. Nature. 2020 Jun; 582(7811): 289-93. doi: 10.1038/s41586-020-2223-y.

[8] Chatterjee S, Maity A, Chowdhury S, Islam MA, Muttinini RK, Sen D. In silico analysis and identification of promising hits against 2019 novel

DOI: https://doi.org/10.54393/fbt.v2i01.23

coronavirus 3C-like main protease enzyme. Journal of Biomolecular Structure and Dynamics. 2021 Sep; 39(14): 5290-303. doi: 10.1080/07391102.2020.1787228.

[9] Shi J and Song J. The catalysis of the SARS 3C-like protease is under extensive regulation by its extra domain. The FEBS Journal. 2006 Mar; 273(5): 1035-45. doi: 10.1111/j.1742-4658.2006.05130.x.

[10] Nashed NT, Kneller DW, Coates L, Ghirlando R, Aniana A, Kovalevsky A, *et al.* Autoprocessing and oxyanion loop reorganization upon GC373 and nirmatrelvir binding of monomeric SARS-CoV-2 main protease catalytic domain. Communications Biology. 2022 Sep; 5(1): 976. doi: 10.1038/s42003-022-03910-y.

[11] Asif M and Khodadadi E. Medicinal uses and chemistry of flavonoid contents of some common edible tropical plants. Archives of Advances in Biosciences. 2013 Jun; 4(3): 119-138. doi: 10.22037/jps.v4i3.4648.

[12] Sepúlveda-Arias JC, Veloza LA, Escobar LM, Orozco LM, Lopera IA. Anti-inflammatory effects of the main constituents and epoxides derived from the essential oils obtained from Tagetes lucida, Cymbopogon citratus, Lippia alba and Eucalyptus citriodora. Journal of Essential Oil Research. 2013 Jun; 25(3): 186-93. doi: 10.1080/10412905.2012. 751556.

[13] Ranitha M, Nour AH, Sulaiman ZA, Nour AH. A comparative study of lemongrass (Cymbopogon Citratus) essential oil extracted by microwave-assisted hydrodistillation (MAHD) and conventional hydrodistillation (HD) Method. International Journal of Chemical Engineering and Applications. 2014 Apr; 5(2): 104. doi: 10.7763/IJCEA.2014.V5.360.

[14] Zakaryan H, Arabyan E, Oo A, Zandi K. Flavonoids: promising natural compounds against viral infections. Archives of Virology. 2017 Sep; 162: 2539-51. doi: 10.1007/s00705-017-3417-y.

[15] Pinto ZT, Sánchez FF, Santos AR, Amaral AC, Ferreira JL, Escalona-Arranz JC, *et al.* Chemical composition and insecticidal activity of Cymbopogon citratus essential oil from Cuba and Brazil against housefly. Revista Brasileira de Parasitologia Veterinária. 2015 Jan; 24: 36-44. doi: 10.1590/S1984-29612015006.

[16] Fokom R, Adamou S, Essono D, Ngwasiri DP, Eke P, Mofor CT, *et al.* Growth, essential oil content, chemical composition and antioxidant properties of lemongrass as affected by harvest period and arbuscular mycorrhizal fungi in field conditions. Industrial Crops and Products. 2019 Oct; 138: 111477. doi: 10.1016/j.indcrop.2019.111477.

[17] Akande IS, Samuel TA, Agbazue U, Olowolagba BL. Comparative proximate analysis of ethanolic and water extracts of Cymbopogon citratus (lemon grass) and four tea brands. Plant Sciences Research. 2011; 3(4): 29-35. doi: 10.3923/psres.2011.29.35.

[18] Dias R, de Azevedo J, Walter F. Molecular docking algorithms. Current Drug Targets. 2008 Dec; 9(12): 1040-7. doi: 10.2174/138945008786949432.

[19] Saif R, Raza MH, Rehman T, Zafar MO, Zia S, Qureshi AR. Molecular docking and dynamic simulation of Olea europaea and Curcuma Longa compounds as potential drug agents for targeting Main-Protease of SARS-nCoV2. ChemRxiv. 2021: 1-22. doi: 10.26434/chemrxiv.13246739.

[20] Okimoto N, Futatsugi N, Fuji H, Suenaga A, Morimoto G, Yanai R, *et al.* High-performance drug discovery: computational screening by combining docking and molecular dynamics simulations. PLoS Computational Biology. 2009 Oct; 5(10): e1000528. doi: 10.1371/journal.pcbi.1000528.